PERMEABILITY PREDICTION FOR SHEARED, COMPACTED TEXTILES DURING LIQUID COMPOSITE MOULDING

Andrew Long, Francois Robitaille, Benjamin Souter and Christopher Rudd
School of Mechanical, Materials, Manufacturing Engineering and Management, University of Nottingham, Nottingham NG7 2RD, UK

SUMMARY: This paper describes an algorithm for the prediction of the planar permeability tensor for general preforms. The porous medium is represented as a series of interconnected channels; the main challenge with this method is to provide an adequate representation of the channel geometry. The implementation discussed here is based on a textile modeller previously developed by the authors. Flow is assumed to occur mainly in the plane of the textile, corresponding to the case of thin preforms. The algorithm reduces the 3D flow domain to a smooth multi-faceted curved surface. This surface describes the channels and corresponds to the streamlines followed by the fluid in the preform. A tow permeability or local gap height is associated to each point of the surface, depending if this point is located inside or outside of a tow. Darcy's law and the analogue equation for flow in a channel are then solved using a standard finite difference technique, and a value of the directional permeability is obtained. The paper describes the main geometric operations involved in the algorithm.

KEYWORDS : Permeability, Preform, Textiles, Liquid Composite Moulding.

INTRODUCTION

A general textile modeller (Fig. 1) has been developed by the authors; the model provides generic geometric definitions of virtually any textile under a simple, unified format [1, 2]. The objective was to provide basic textile geometries that could be used in integrated simulations. For example, the configuration taken by a dry textile when it is draped and compacted could be calculated with appropriate methods. Also, provided that a complementary mesh is added for the zones extending between the tows, the model can be use as a basis for the prediction of the mechanical properties of textile composites. Such work is currently in progress [3]. Here the model is used as a basis for the calculation of the permeability of the preforms [4-7].

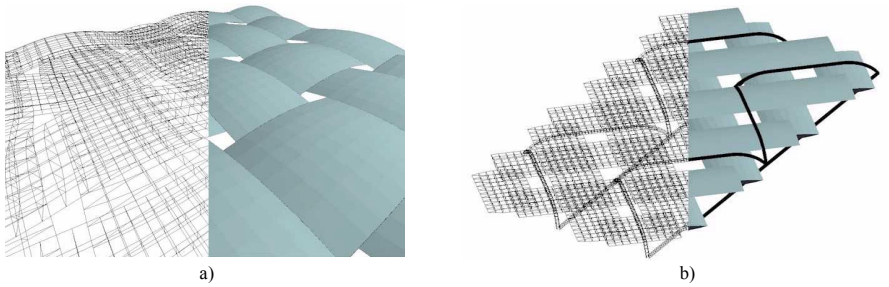

Fig. 1. Images and 3D meshes of typical textiles obtained from the TexGen software developed by the authors [1, 2]; a) plain weave, b) ±45° stitched.

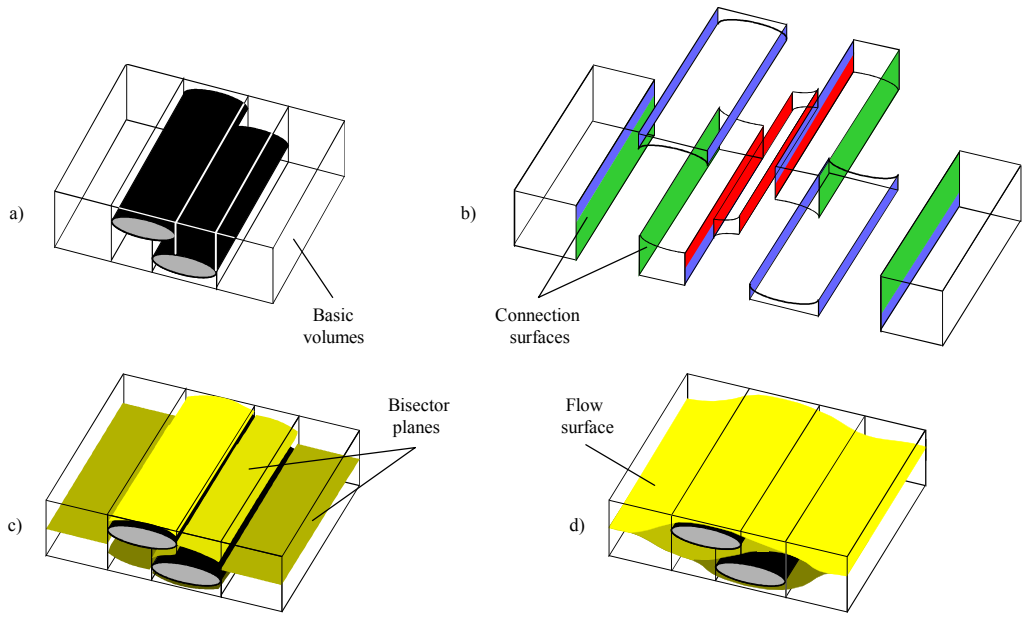

Fig. 2. Basic geometric steps of algorithm; a) Tows and basic volumes, b) Connections of basic volumes, c) Bisector planes, d) Connected bisector planes.

The basic idea is described as follows (Fig. 2). The free volume extending around the tows and other entities present in the flow domain is separated in basic volumes. Basic volumes are continuous volumes that feature vertical walls and are delimited by a single entity (tow or domain boundary) on each of their lower and higher surfaces (Fig. 2a). When the basic volumes are created, the connection surfaces are noted. Connection surfaces are surfaces that are coplanar in the flow domain but are associated to different, neighbouring basic volumes (Fig. 2b). Then the bisector planes are created. A bisector plane separates each basic volume into two parts of equal volume along the vertical (Fig. 2c); the bisector planes represent the surface along which the fluid is generally assumed to flow through a basic volume. Finally the bisector planes are connected into one smooth, multi-faceted surface (Fig. 2d); the information provided by the configuration of the connecting surfaces is used at this stage. The next steps consist of meshing the flow surface and applying appropriate boundary conditions.

The above steps automatically create a surface which correspond to the streamlines that one would draw instinctively in order to represent the flow field in a fairly open, or low v_f, configuration. Most textile structures or combinations of layers can be processed. However, real preforms always feature contact between the tows. The tows and textile layers are often heavily deformed and their shapes differ significantly from the ideal, generic ones shown in Figs. 1, 2. The algorithm includes supplementary steps that account for this; hence an actual preform can be processed, provided that the definition of its geometry is available (Fig. 3).

Once the basic volumes and the first bisector planes are identified, the algorithm identifies zones of the basic volumes where their thickness is close to zero (Fig. 3e). The perimeters of these zero-thickness zones are then projected and compared; superimposition zones are identified (Fig. 3f). Then the volumes which are associated to tows and extend continuously

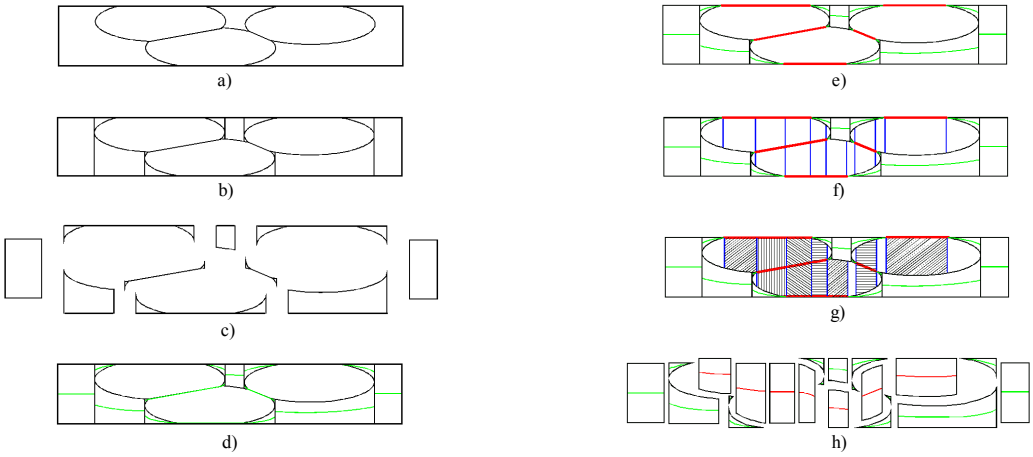

Fig. 3. Supplementary geometric steps of algorithm, accounting for deformed and contacting tows. a) to d) see Fig. 2; e) Zero-thickness zones in basic volumes, f) Projections of zero-thickness zones, g) Merging of tow volumes, h) Creation of bisector planes.

between superimposed zero-thickness zones are merged (Fig. 3g). Finally, bisector planes are created for the merged volumes, and are connected with those created previously (Fig 3h).

The second part of the algorithm automatically identify zones of the preform where the fluid cannot flow through an open channel; only under such circumstances is it likely that the fluid will flow inside the less permeable tows. Hence the localisation of high flow rates zones is partially done by the geometric algorithm, and it is completed by the numerical FD solution.

In principle, the algorithm as defined above can indifferently process most configurations encountered in actual preforms including compacted tows, sheared textiles, multiple-layers preforms, etc.; calculations can also be done over curved domains. In order to simplify the presentation, only single textile layers defined in a flat domain of constant thickness are considered below. Whilst the case of curved domains complicates the mathematical treatment, the other restrictions can be lifted easily. Also, Fig. 4 shows tows that can and cannot be processed at this stage; again the limitations were brought in only for simplification purposes.

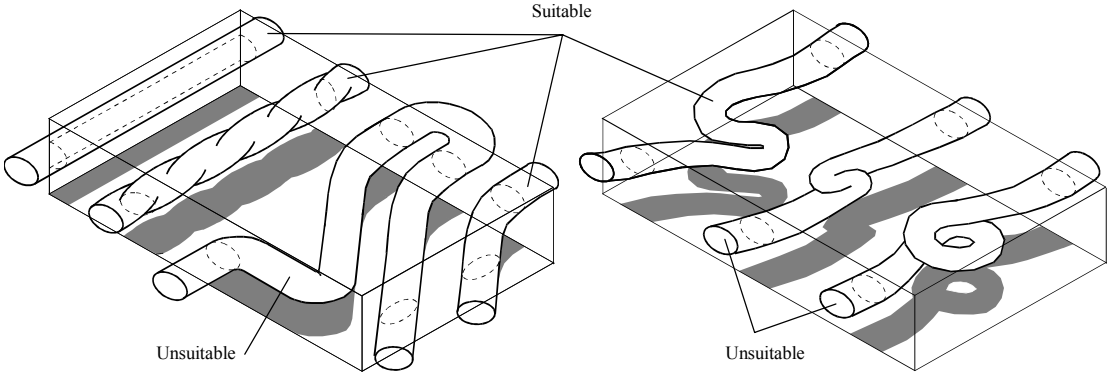

Fig. 4. Presently, tows re-entering the domain (a) and tows superimposing on themselves (b) cannot be processed; all other cases are suitable.

ALGORITHM

The first operation is the definition of the lower and higher tow surfaces and lateral tow edges (Fig. 5). Tows are defined as distinct ensembles of three-node elements, each forming a continuous open-ended outer envelope extending beyond the boundaries of the domain. The elements in each ensemble are separated into two groups corresponding to the lower and higher tow surfaces. The surfaces are delimited by two common lateral tow edges; these are the two continuous series of element edges that lie furthest from the centreline on each side of a tow in the preform mid-plane. Arbitrary start and end points are associated with each tow; these allow the identification of a left and a right tow edge. In addition to the left and right tow edges, numeral co-ordinate data are stored for the left edge start, left edge end, right edge start and right edge end, but not for the centrelines. The left and right edge starts lie at the same extremity of the tow, and the left and right edge ends lie at the other extremity.

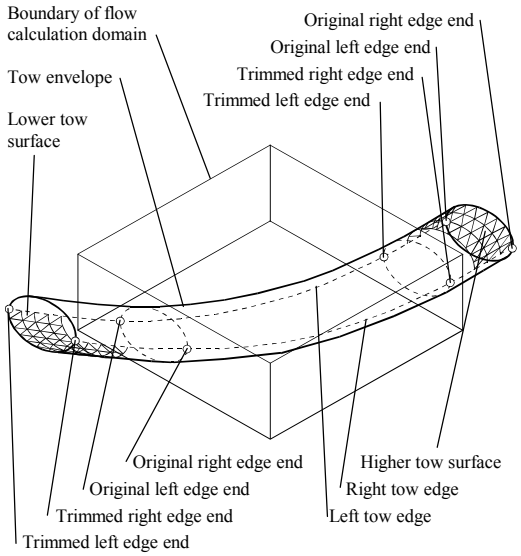

Fig. 5. Lower and higher surfaces, lateral tow edges, left/right start/end points.

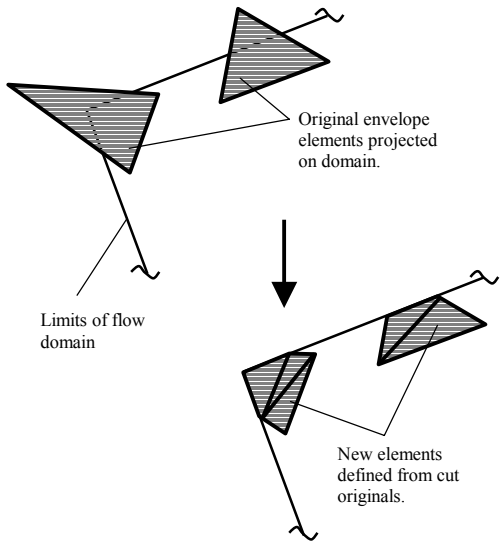

Fig 6. Trimming of typical elements crossing domain boundaries.

The second operation consists of trimming the textile to the boundaries of the flow domain. This is straightforward as the elements making the tow surfaces are triangular. Those located in the domain are kept unchanged, those located entirely out of the domain are removed, and those crossing the boundaries of the domain are split into one or more new triangular elements located in the domain. This last operation involves the creation of new nodes located on the boundary of the flow domain (Fig. 6).

The third operation consists of identifying control points for each pair of tows present in the domain. Control points are defined in the *x, y* plane as the positions where projection of the 4 lateral tow edges coincide; left and right edges starts and ends and the corners of the flow domain are also included (Fig. 7). Most of the former points simply correspond to crossovers of two lateral edges. However, because of the nature of textile processes, parallel projections of lateral tow edges cannot be neglected. Hence simple crossovers are identified as crossover control points while points delimiting a line where two projections superimpose are identified

as collinear control points. In this case some numerical criterion is used to assess if the projections of two edges are effectively collinear. This operation is done for each pair of tows.

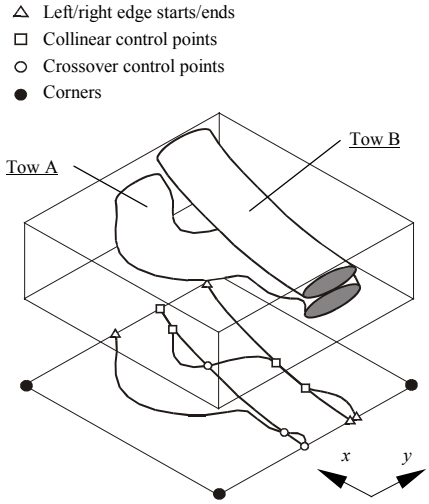

Fig. 7. Control points: edge starts/ends, collinear and crossover points.

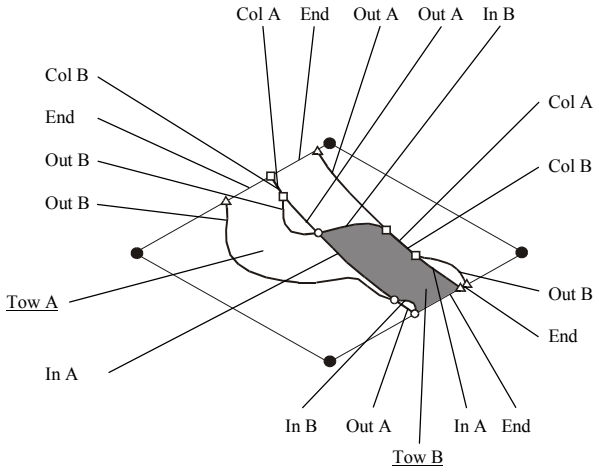

Fig 8. Superimposition surface and edge segments.

The fourth operation consists of identifying superimposition surfaces for each pair of tows. Superimposition surfaces are continuous zones of the *x, y* plane where the projection of two tows intersect; there is no limit to the number of distinct superimposition surfaces that can be defined for two given tows A and B. This operation is achieved by splitting each lateral tow edge into edge segments extending between two control points (Fig. 8). Edge segments from tow A are tagged as being inside or outside of tow B, or collinear to one of its lateral edges; edge segments from tow B are identified similarly relatively to tow A. Superimposition surfaces (shaded in Fig. 8) are easily identified as their perimeter must be closed and extend along edge segments that are inside a tow or collinear with one of its edges ("In" and "Col" in Fig. 8), or along tow ends defined on the domain boundary ("End" in Fig. 8). The superimposition surfaces are stored as *x*, *y* co-ordinates of points located on their perimeter, i.e. the relevant control points and node projections. The information stored also identifies the two relevant tows, and the two 3D tow surfaces effectively facing each other over the domain; here for example, these are the higher surface of tow A and lower surface of tow B. Finally the co-ordinates of the control points are associated to each lateral edge and stored as such.

The fifth operation consists of identifying void surfaces for each pair of tows. Void surfaces are continuous zones of the *x*, *y* plane where no tow projection is present; there is no limit to the number of distinct void surfaces that can be defined for two given tows A and B. Void surfaces (shaded in Fig. 9) are identified as their parameters must be closed and extend along edge segments that are outside a tow or collinear with one of its edge ("Out" and "Col" in Fig. 9), or along the domain boundary. The void surfaces are stored as *x*, *y* co-ordinates of points located on their perimeter; the information stored also identifies the two relevant tows.

The sixth operation consists of creating the first basic volumes, namely those defined between

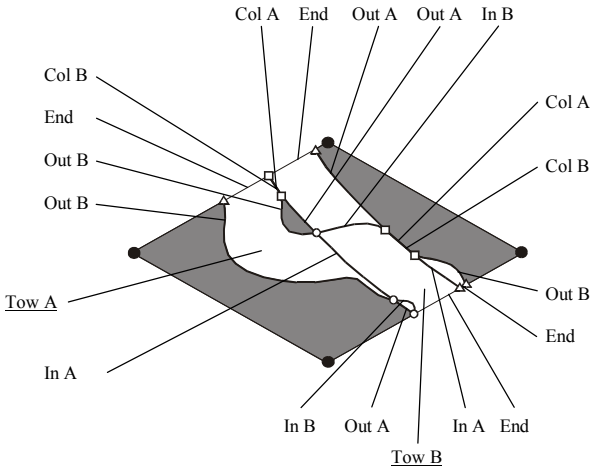

Fig. 9. Void surfaces and edge segments.

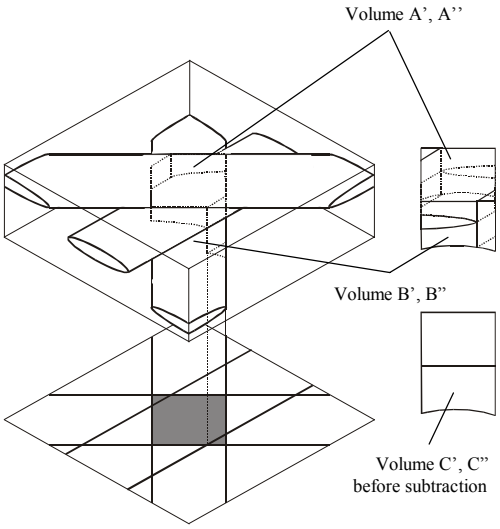

Fig 10. Basic volumes between a lower and a higher tow surface.

the lower surface of a tow and the higher surface of another tow. The 3D surfaces associated with the superimposition surfaces defined above are used. Surfaces of both types are located at the same position in the *x*, *y* plane; the associated 3D surfaces are coplanar with the lower and higher surfaces of the tows. Each couple of associated 3D surfaces is considered in turn.

Firstly, couples of 3D surfaces A' and A" (associated to superimposition surface A) between which no other 3D surfaces B' or B" (associated to any other superimposition surface B) can be found are identified. These surfaces A' and A" are identified by verifying that the 3D surfaces B' and B" of which the superimposition surface B intersects the superimposition surface A (in the *x*, *y* plane) are not defined between A' and A" (along *z*). This is easily done as the identity of the tow surfaces associated to each superimposition surface was stored in step 4, and the definitions of the tow surfaces are available from step 1. The volume defined between the 3D surfaces A' and A" is a basic volume; when such a volume is created the 3D surfaces are tagged as being part of a volume, and the relevant information is stored (Fig. 10).

Secondly, couples of 3D surfaces C' and C" between which the only 3D surfaces that can be found are already part of a volume (such as A', A") are identified using a similar process. In order to create basic volumes (one or more) the superimposition surface A must be subtracted from the superimposition surface C. This is straightforward; there is no theoretical limitation to the number of independent basic volumes that can be created between C' and C" by the subtraction. The algorithm also handles cases where two couples of surfaces A', A" and B', B", both forming independent basic volumes, must be subtracted from the volume defined between C' and C"; there is no theoretical limitation to the number of such couples which may have to be subtracted simultaneously from a larger volume enclosing them (Fig. 10).

One last remark is made regarding the operation detailed in the above paragraph. When a volume such as the one defined between C' and C" is created, all the volumes enclosed in it (such as the one defined between A' and A") are tagged as enclosed volumes. If a third

volume D', D" is defined around C, C", then only this one (C', C") must be subtracted from D', D". The initial volume A', A" does not affect the process anymore, and the couple of surfaces A' and A" can be bypassed altogether. When investigating a pair of 3D surfaces, only the largest or outermost volumes defined between them need to be considered.

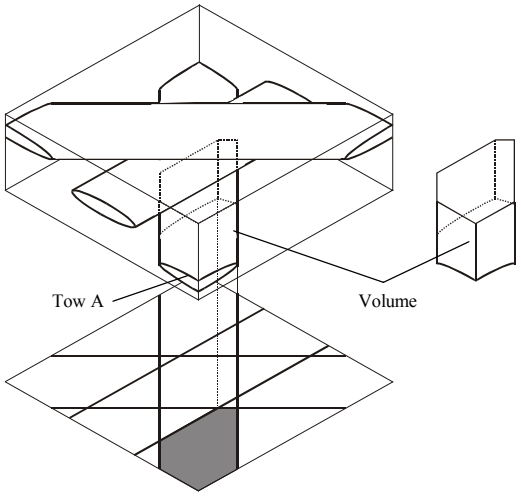

Fig. 11. Basic volumes defined between a tow surface and a horizontal wall.

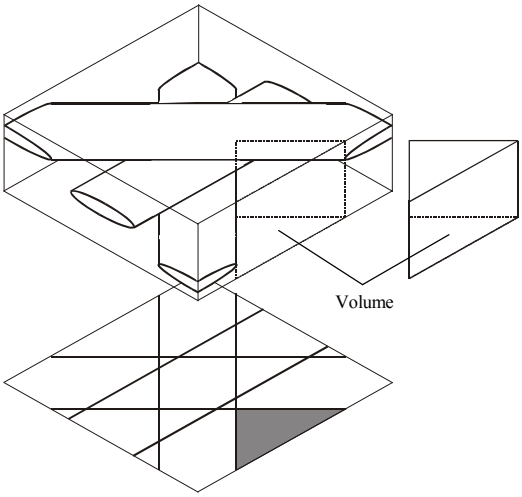

Fig 12. Basic volumes defined between two horizontal walls.

The seventh operation consists of creating the basic volumes that are defined between a tow and a horizontal domain wall. These volumes can appear next to a tow surface that is nearest of a horizontal wall, or on both sides of a tow in a zone where no superimposition occurs. Here all lower and higher tow surfaces are considered once, in turn. Superimposition surfaces involving the relevant side of tow A, which were identified in step 4, are subtracted from the projection of the entire tow A in the x, y plane. Basic volumes are defined directly between the remaining zones of the lower or higher surface of tow A and the appropriate horizontal wall. There is no theoretical limit to the number of such volumes that can be defined between a tow and a wall; the volumes are identified and stored as mentioned above (Fig. 11).

The eighth operation is the last one where basic volumes are created. Here volumes involving only the top and bottom horizontal walls of the domain are created; these volumes correspond to holes appearing along the z axis, throughout the preform. The relevant surfaces are easily created by identifying the intersection of all the void surfaces, which were created in step 5; there is no theoretical limit to their number. The basic volumes are simply defined over these intersections, between the horizontal walls. The volumes are identified and stored (Fig. 12).

At this stage all basic volumes defined between the tows are available; the ninth operation consists of creating the individual bisector planes for each volume. This conceptually simple operation involves practical aspects. As mentioned in step 1 the algorithm uses tow envelopes that are defined from triangular elements. The objective of the geometrical part of the algorithm is to create one smooth, multi-faceted surface over which a mesh is generated and solved. In a context where the tow shapes will eventually be obtained via methods such as

structural finite elements, envelopes containing a large number of elements can be envisaged. Creating the bisector planes as surfaces which rigorously separate the basic volumes in two equal parts along z at each x, y co-ordinate will translate nodes associated to both the lower and higher surfaces of the volumes into the new surface, and result in a consequent number of new triangular surfaces; this is not appropriate to the solution. Instead, the algorithm selects a number of nodes based on a general density of nodes selected by the user and on the size of the bisector plane to be built. In doing so the algorithm can re-equilibrate the density of the mesh along two arbitrary directions (Fig. 13).

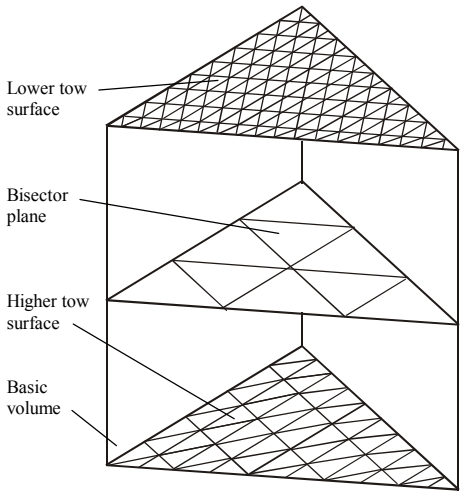

Fig. 13. Generation of bisector plane from initial tow envelopes.

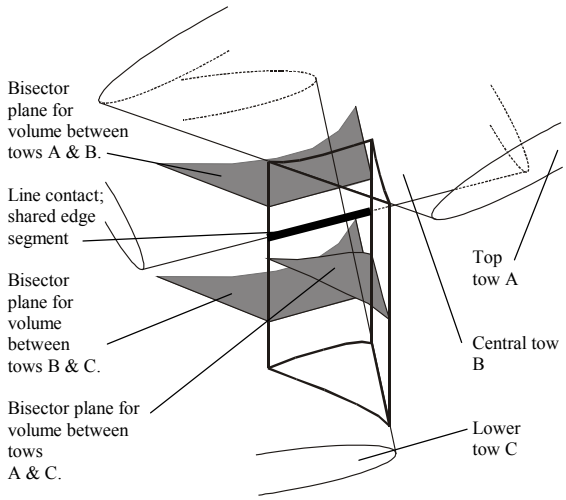

Fig 14. Bisector planes and connections to be made between them.

The tenth operation performed by the algorithm consists of identifying the connections to be made between the bisector planes associated to neighbouring volumes. Basic volumes extend between a lower and a higher tow surface. These surfaces and the x, y co-ordinates of their corners are identified when the volumes are created; the volume actually extends between the two tows which are furthest apart among those to which the control points forming the corners of the surfaces are associated. All other contacting tows positioned between these two along z interact with the volumes on a line contact. The line contacts are defined on lateral tow edges, with their ends located at the same x, y co-ordinates where the relevant control points are found (Fig. 14). Therefore after formally identifying the lateral surfaces of each volume, contacts can be identified simply by considering the control points defined on the projections of lateral tow edges; neighbouring volumes will share at least a segment on one common tow edge.

At this stage the basic volumes and the connections to be made between them are identified. As mentioned above (Fig. 3), the eleventh step consists of identifying tow volumes for which bisector planes are to be created and connected to the other bisector planes created at step 9. The creation of these bisector planes involves a number of operations that are somewhat similar those previously described. Consequently this part of the algorithm is described in a more general manner; references can be made to the above paragraphs.

Firstly, zones in the initial basic volumes featuring near-zero thickness are identified. This operation is performed by looking at the normal distance separating partially superimposed elements of the bottom and top surfaces. The distance can be calculated in a number of ways and in each case, different criteria can be applied. One way of assessing the normal distance for an element A consists in identifying the elements B, C and D (some of which may be the same) that intersect the normal to each node of element A, and calculating the average distance between the nodes and the elements. On each surface, zero-thickness zones extend on contiguous elements as long as the above distance criterion is satisfied. There is no theoretical limitation to the number of zero-thickness zones that can be identified on one bottom or top surface, for one volume. The algorithm performs a number of additional operations such as merging neighbouring zero-thickness zones, in order to simplify further processing. The final zero-thickness zones are stored as *x*, *y* perimeters and associated to the relevant basic volumes.

Once the zero-thickness zones are identified they are investigated in turn for superimposition along *z*. This is a more straightforward operation than the one described in steps 3 and 4, as the zero-thickness zones are readily defined as closed perimeters. The objective is to create basic tow volumes that expand in the space occupied by the tows, below or above at least one zero-thickness zone; this operation is represented in Figs. 3f and 3g. The volumes that are defined immediately above or below one such surface, or continuously between two or more such surfaces, are merged into one basic tow volume. If, for example, one zero-thickness zone A superimposes totally with a zero-thickness zone B and partially with another zero-thickness zone C, then one basic tow volume will be created between zero-thickness zones A and C and another adjacent zero-thickness zone will appear between zero-thickness zones A and B (Fig. 15). Once the basic tow volumes are available, bisector planes are created as described in an operation similar to step 9. Then the connections to be made between these bisector planes and the ones defined for the basic volumes are identified in an operation similar to step 10.

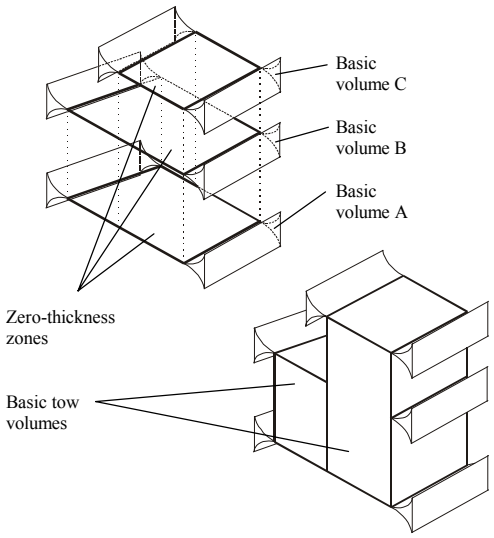

Fig. 15. Superimposition of zero-thickness zones and basic tow volumes.

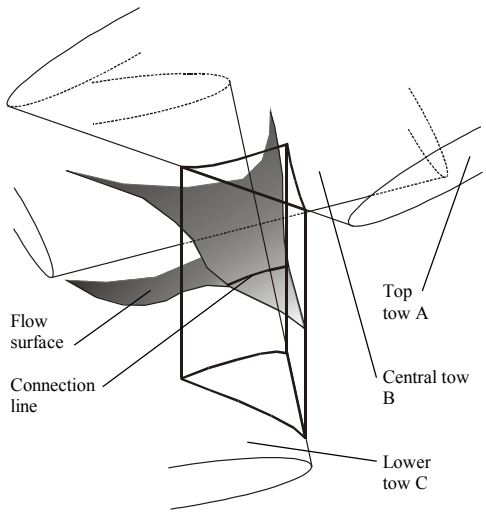

Fig 16. Connection line between basic volumes.

The operations performed after the above 11 steps consist of creating the connection lines, which are 3D curved lines along which the different bisector planes connect (Fig. 16), creating the connected flow surface, and meshing it. The latter operations are performed using b-splines [8] and standard finite differences mesh generation [9]. Mesh nodes located on the connection lines are created first; then a curvilinear mesh is created for each patch, and the individual meshes are connected. At this stage the geometric work is complete; a standard finite difference method is used to solve the equations for saturated flow over the domain.

CONCLUSION

This paper presents the geometric operations involved in the automatic processing of a textile preform over a limited flow domain, for the calculation of components of the in-plane permeability tensor. The tow envelopes used as an input can be provided under a large number of configurations; hence the algorithm can process the cases of sheared and compacted, contacting tows indifferently. The current solution involves Darcy's law and analogue expressions for flow between infinite plaques, for a saturated domain; other equations may eventually be implemented in order to simulate unsaturated flow and phenomena such as void entrapment.

ACKNOWLEDGEMENTS

The continuing support of the Ford Motor Company Limited, Dowty Aerospace Propellers Limited, Rolls Royce Plc, Brookhouse Paxford Limited, Flemings Industrial Fabrics and the Engineering and Physical Sciences Research Council, UK, is gratefully acknowledged.

REFERENCES

1. Robitaille, F., Clayton, B.R., Long, A.C., Souter, B.J. and Rudd, C.D., "Geometric Modelling of Industrial Preforms: Woven and Braided Textiles", *Proceedings of the Institution of Mechanical Engineers*, 1999, Vol. 213, Part L, pp. 69-83.

2. Robitaille, F., Clayton, B.R., Long, A.C., Souter, B.J. and Rudd, C.D., "Geometric Modelling of Industrial Preforms: Warp-Knitted Textiles", *Proceedings of the Institution of Mechanical Engineers*, 2000, Vol. 214, Part L, pp. 71-90.

3. Crookston, J.J., Souter, B.J., Long, A.C. and Jones, I.A., "The Application of a General Fibre Architecture Model for Composite Mechanical Property Prediction", *Proceedings of ICCM-13*, 2001, Beijing, China.

4. Scheidegger, A.E., "The Physics of Flow Through Porous Media", University of Toronto Press, 3rd Edition, Toronto, Canada, 1974.

5. Dullien, F.A.L., "Porous Media: Fluid Transport and Pore Structure", Academic Press, New York, USA, 1979.

6. Bear, J., "Dynamics of Fluids in Porous Media", Elsevier, New York, USA, 1974.

7. Nield, D.A. and Bejan, A., "Convection in Porous Media", Spinger-Verlag, New York, USA, 1992.

8. Faux, I.D. and Pratt, M.J., "Computational Geometry for Design and Manufacture", Ellis Horwodd Ltd., Chichester, UK, 1979.

9. Thompson, J.F., Warsi, Z.U.A. and Mastin, C.W., "Numerical Grid Generation", North Holland Ltd., New York, USA, 1985.